
NTKCPL: Active Learning on Top of Self-Supervised Model by Estimating True Coverage

Ziting Wen

University of Sydney
zwen4889@uni.sydney.edu.au

Oscar Pizarro

University of Sydney
Norwegian University of Science and Technology
oscar.pizarro@ntnu.no

Stefan Williams

University of Sydney
stefan.williams@sydney.edu.au

Abstract

High annotation cost for training machine learning classifiers has driven extensive research in active learning and self-supervised learning. Recent research has shown that in the context of supervised learning different active learning strategies need to be applied at various stages of the training process to ensure improved performance over the random baseline. We refer to the point where the number of available annotations changes the suitable active learning strategy as the phase transition point. In this paper we establish that when combining active learning with self-supervised models to achieve improved performance, the phase transition point occurs earlier. It becomes challenging to determine which strategy should be used for previously unseen datasets. We argue that existing active learning algorithms are heavily influenced by the phase transition because the empirical risk over the entire active learning pool estimated by these algorithms is inaccurate and influenced by the number of labeled samples. To address this issue, we propose a novel active learning strategy, neural tangent kernel clustering-pseudo-labels (NTKCPL). It estimates empirical risk based on pseudo-labels and the model prediction with NTK approximation. We analyze the factors affecting this approximation error and design a pseudo-label clustering generation method to reduce the approximation error. We validate our method on five datasets, empirically demonstrating that it outperforms the baseline methods in most cases and is valid over a wider range of training budgets.

1 Introduction

The boom in deep learning models in recent years stems in part from the massive amounts of data available for training these models [11, 17, 23]. However, the demand for large amounts of data, especially labeled data, in turn, constrains the application of deep learning models, since large numbers of labels imply high annotation costs when considering a new dataset [41, 1, 45]. Active learning is a path to alleviate the cost of labeling by selecting informative subsets of samples to annotate, thereby accelerating the learning rate.

However, the benefits of active learning have been increasingly questioned in recent years [25, 28]. One of the main concerns is that training a model initialized by self-supervised learning with randomly selected labeled samples often yields results far beyond those obtained by existing active learning with supervised training (randomly initialized or initialized by the last round of the active learning model) [6, 8, 7, 14, 9]. Because the latter only uses labeled data to train the network, while the

former uses a large amount of unlabeled data to train the backbone of the network. Since most existing active learning algorithms are designed in the context of supervised training, they must be validated with a large number of labels compared to the number of labels required in training from a self-supervised model. This means that the effectiveness of these active learning algorithms is not guaranteed in the case of having access to relatively few annotations, as is the case when combining with a self-supervised model. Several studies [15, 42, 4] have shown that many existing active learning strategies fail to outperform the random baseline when combining them with self-supervised learning. In this paper, we focus on designing an active learning strategy that works well in concert with a self-supervised model.

The “phase transition” phenomenon [15] is known to occur in active learning with supervised training. It refers to the fact that an active learning strategy that outperforms a random baseline when the total number of labels is small will be inferior to a random baseline when the total number of labels is large (called the **low-budget** strategy) and vice versa (called the **high-budget** strategy). We note that when combining active learning with the self-supervised model, the cut-off point between low-budget and high-budget strategy occurs much earlier. For example, in the CIFAR-100 [21], the cut-off point is about 10,000 labeled samples when training in the supervised learning way [16]. But, the cut-off point shifts forward to about 1,500 labeled samples when training from a self-supervised model. The forward-moving cut-off point means that even if the annotation budget is low (only one order of magnitude above the number of classes in the dataset), it is likely to hit that cut-off point. Thus, for a previously unseen dataset, it is difficult to simply determine whether a low-budget or high-budget strategy should be chosen since the difficulty varies from dataset to dataset. In this paper we use this problem to motivate the design of an active learning strategy with a wider effective budget range.

Since existing low-budget strategies are designed based on the idea of feature space coverage [24, 15, 42], we first analyze the problems of determining coverage based on sample feature distances in sec. 2. After that, we propose that the true coverage where the empirical risk is zero, can be estimated based on pseudo-labels and predictions of the model trained on the candidate set. Based on this, we propose our active learning strategy, Neural Tangent Kernel Clustering-Pseudo-Labels (NTKCPL), which uses the NTK [18, 27] and CPL to approximate empirical risk on active learning pool in sec. 3.2. And we analyze which factor affects approximation error in sec. 3.3. Based on this analysis, we design a CPL generation method in sec. 3.4. Extensive experimental results demonstrate that our method outperforms state-of-the-art approaches in most cases and has a wider effective budget range. As part of the results (sec. 4) we also show our method is effective for self-supervised features of different quality.

Our contribution is summarized as follows: (1) We propose a novel active learning strategy, NTKCPL, by estimating empirical risk on the whole active learning pool based on pseudo-labels. (2) We analyze the approximation error of the empirical risk in the active learning pool when NTK and CPL are used to approximate networks and true labels. (3) Our method outperforms both low- and high-budget active learning strategies within a range of annotation quantities one order of magnitude larger than traditional low-budget active learning experiments. This means that our approach can be used more confidently for active learning on top of self-supervised models than existing low-budget strategies.

1.1 Related Work

Most active learning strategies are designed and validated in the high-budget scenario where network weights are randomly initialized or initialized from the weights of the previous active learning round. Active learning methods mainly include uncertainty-based sampling [22, 13, 19], feature space coverage [32, 24, 42, 33, 5, 40], the combination of uncertainty and diversity [41, 3], learning-based methods [43], and so on [34, 35]. Moreover, some recent studies explore “**look ahead**” strategies [26, 38], where samples are selected based on the model trained on candidate training sets. However, with the development of self-supervised training, the training approach for low-budget scenarios has shifted to training based on a self-supervised pre-trained model [24]. This change in the training method implies a shift in the total number of samples that need to be selected by active learning. When training based on a self-supervised model, often only 0.4-6% of the total data needs to be labeled to achieve similar results to training with 20-40% labeled data on a randomly initialized network [4]. Recent studies have shown that there exists a phase transition phenomenon in active learning strategies, whereby opposite strategies should be adopted in high-budget and low-budget scenarios [15], causing many active learning strategies designed for high-budget scenarios unsuitable

for training based on a self-supervised model. As a result, recent studies have explored active learning strategies specifically designed for low-budget scenarios [15, 42, 31, 20]. However, we find that these strategies are effective only when the number of labeled data samples is extremely small, and as we increase the labeled data to one order of magnitude above the number of classes of the dataset, their performance falls below that of the random baseline.

2 Insight: Distance is not an accurate indicator of empirical risk

The goal of the active learning is to find a labeled subset, $D_C = (x_i, y_i)_{i=1}^{N_C}$, such that the model trained on that subset, f_{D_C} , has the minimized empirical risk in the entire active learning pool, $D = (x_i, y_i)_{i=1}^N$ as shown in eq. 1.

$$\operatorname{argmin}_{D_C} \frac{1}{N} \sum_{i \in D} \operatorname{Loss}(f_{D_C}(x_i), y_i) \quad (1)$$

Unfortunately, during active learning, we do not have the labels of the entire active learning pool, so we cannot compute this loss directly. To address this problem, current methods [32, 24, 33] covert empirical risk minimization into feature space coverage based on Lipschitz continuity. Although Lipschitz continuity guarantees that the difference between the model’s predictions is less than the product of the Lipschitz constant and the difference between inputs, it does not guarantee that their predictions fall into the same class. In practice, we cannot determine the true coverage because we do not know the distance threshold beyond which the model would change its predicted class for unlabeled samples.

Therefore, the current solution is to minimize the coverage radius assuming full coverage [32] or to maximize coverage based on high purity coverage [42], where purity refers to the probability that the sample has the same label within a given distance. Assuming full coverage leads to an overestimated coverage as shown in fig. 1a, i.e., some covered samples still have a large empirical risk, while high-purity coverage causes underestimated coverage as shown in fig. 1b. The overestimated coverage may cause the active learning algorithm to miss samples in areas that are not truly covered, while underestimated coverage makes active learning algorithms likely to select redundant samples. These affect the performance of active learning.

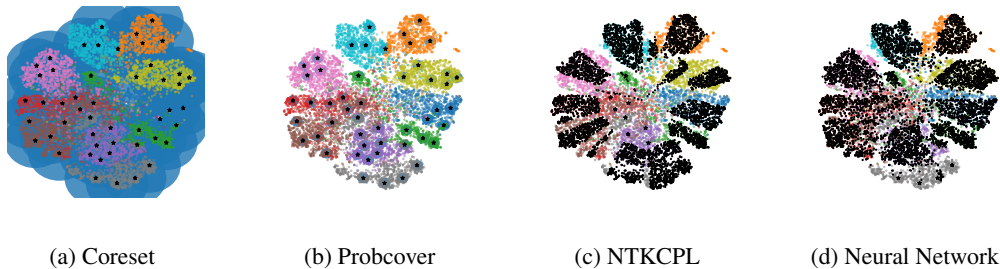


Figure 1: Coverage estimation based on sample feature distance vs. NTKCPL. Here different colors represent different categories, the black star denotes labeled samples and the blue circle represents the samples considered covered based on the feature distance approach. Coreset assumes full coverage and Probcover assumes high purity coverage. The coverage estimated by our method, NTKCPL, and true coverage based on predictions of the neural network is represented by black dots. The coverage estimated by NTKCPL is more consistent with the true coverage of the neural network than those estimated based on feature distances.

Additionally, estimating the empirical risk based on distance implies the assumption that model predictions are only relevant to the nearest labeled sample, which is often not the case in reality. To estimate the true coverage, we propose a new strategy, NTKCPL. It estimates the empirical risk based on the predictions of the model trained on the candidate set and pseudo-labels.

3 Method: NTKCPL

In sec. 3.1, we briefly review the Neural Tangent Kernel (NTK) [18] that enables active learning strategies based on the outputs of a model trained on a candidate set feasible. Then, we propose our active learning strategy, NTKCPL, in sec. 3.2 and analyze the approximation error of NTKCPL in sec. 3.3. Finally, based on the analysis, we introduce the method of generating cluster pseudo-label in sec. 3.4.

3.1 Preliminaries

Neural Tangent Kernel (NTK) is a powerful tool to analyze the training dynamics of neural network. Jacot et al. [18] show that the neural network is equivalent to the kernel regression with Neural Tangent Kernel when network is sufficiently wide and its weights are initialized properly [2]. The NTK, \mathcal{K} , is shown in eq. 2, where the f denotes a neural network with parameters θ and \mathcal{X} denotes training samples. When training with MSE loss, the neural network has a closed-form solution for the prediction of test sample x at iteration t as eq. 3, where \mathcal{Y} denotes labels of trainset and f_0 denotes the output of network with initialized weights.

$$\mathcal{K}(\mathcal{X}, \mathcal{X}) = \nabla_{\theta} f(\mathcal{X}) \nabla_{\theta} f(\mathcal{X})^T \quad (2)$$

$$f_t(x) = f_0(x) + \mathcal{K}(x, \mathcal{X}) \mathcal{K}(\mathcal{X}, \mathcal{X})^{-1} (\mathcal{I} - e^{-t\mathcal{K}(\mathcal{X}, \mathcal{X})}) (\mathcal{Y} - f_0(\mathcal{X})), \quad (3)$$

Additionally, for active learning scenarios, Mohamad [26, 27] proposes the computation time of using NTK can be further reduced by considering the block structure of the matrix, which means that look ahead type active learning strategies can be implemented in a reasonable amount of time. For example, as shown in [26], if we want to use the look ahead active learning strategy, each active learning cycle takes 3 hours to train the entire network of 15 epochs on the MNIST dataset, while it takes only 3 minutes to use NTK with a block structure.

3.2 Framework

We propose a look ahead strategy, NTKCPL, to approximate the empirical risk on the whole active learning pool directly. There are two challenges: (1) estimate empirical risk without labels and (2) estimate predictions of models trained with candidate sets efficiently and accurately.

For the first challenge, clusters on self-supervised features provide good pseudo-labels. Because most samples in the same cluster have the same label [39]. And when the number of clusters is increased, it can improve the purity of clusters, where purity refers to the probability that the sample has the same label within the same cluster. We call these clusters clustering-pseudo-labels (CPL), y_{cpl} .

For the second challenge, as introduced in sec. 3.1, NTK approximates the network well for random initialization and the computation time is acceptable. However, in our scenario, training on top of the self-supervised model, NTK does not approximate predictions of the whole network well. The main reason is that weights of the neural network are initialized by self-supervised learning rather than NTK initialization, i.e., drawn i.i.d. from a standard Gaussian [18]. In addition, the self-supervised initialization provides the neural network with a powerful feature representation capability that is not available in NTK. This leads to inconsistency between NTK predictions and network outputs. So, in our method, the NTK is used to approximate the classifier instead of the whole network. And the inputs of NTK are self-supervised features. Accordingly, we choose a training method following [24] that freezes the encoder initialized by self-supervised learning and trains only the MLP as a classifier. That training method achieves better or equal performance than fine-tuning the whole network in the low-budget case while its prediction is more consistent with the results of NTK. We denote the predictions of NTK with trainset D_C as \hat{f}_{D_C} . Now, the active learning goal in eq. 1 is approximated as eq. 4.

$$\operatorname{argmin}_{D_C} \frac{1}{N} \sum_{i \in D} \operatorname{Loss}(\hat{f}_{D_C}(x_i), y_{cpl,i}) \quad (4)$$

The algorithm is shown in Alg. 1. For computational simplicity and without loss of generality, we use 0-1 loss to calculate empirical risk in eq. 4. In each round of active learning, after computation of NTK based on eq. 2 and generation of CPL based on the method introduced in sec. 3.4, the sample that minimizes the empirical risk on the whole active learning pool after adding labeled set is selected.

Algorithm 1 NTKCPL

1: **Input:** self-supervised feature f_{self} , active learning feature f_{al} labeled set L , unlabeled set U , budget b , initial budget b_0 , maximum cluster number C_{max} , model prediction $Y_{pre,t-1}$ at the last active learning round
2: **Output:** labeled set L , model prediction $Y_{pre,t}$ at this round
3: **if** L is \emptyset **then**
4: $Y_{cpl} \leftarrow$ K-means(f_{self} , b_0)
5: **else**
6: $N_{clu} = \min\{b_i/2, C_{max}\}$
7: $Y_{cpl} \leftarrow$ CPL generation(f_{al} , $Y_{pre,t-1}$, b_0 , N_{clu} , L) based on Alg. 2
8: **end if**
9: Initialize classifier, MLP, compute f_0 and ker based on eq. 2
10: **for** $itr = 1$ **to** b **do**
11: $Emp_risk = []$
12: **for** $(x_i, y_{cpl,i})$ **in** U **do**
13: Compute $Y_{NTK} = \hat{f}(ker, f_0, L \cup (x_i, y_{cpl,i}), U)$ based on eq. 3
14: $Emp_risk += [0-1Loss(Y_{NTK}, Y_{cpl})]$
15: **end for**
16: $i' = \operatorname{argmin} Emp_risk$
17: $L = L \cup (x_{i'}, y_{cpl,i'}), U = U \setminus x_{i'}$
18: **end for**
19: Query label $y_{i', \dots, b}$ of $x_{i', \dots, b}$
20: $L = L \cup (x_{i', \dots, b}, y_{i', \dots, b}), U = U \setminus x_{i', \dots, b}$
21: Train classifier f_t on L
22: model prediction $Y_{pre,t} = f_t(U)$

3.3 NTKCPL Approximate Error

In this section, we analyze what affects the accuracy of NTKCPL estimates of empirical risk on the whole active learning pool. The difference between the true empirical risk and the estimated empirical risk using NTK and CPL is shown in eq. 5. The approximation error can be divided into two terms, the first one is the difference between NTK and neural network prediction, $error_{NTK}$, and the second one is the difference caused by CPL during NTK estimation, $error_{CPL}$. For the $error_{NTK}$, as we mentioned in sec. 3.2, NTK is used to approximate the classifier only to obtain better consistency. To analyze $error_{CPL}$, we start with the relationship between the predictions of NTK trained with the ground truth, $\hat{f}_y(x_i)$, and CPL, $\hat{f}_{cpl}(x_i)$.

$$\begin{aligned} & \frac{1}{N} \sum_{i \in D} \left| Loss(f(x_i), y_i) - Loss(\hat{f}(x_i), y_{cpl,i}) \right| \\ & \leq \frac{1}{N} \sum_{i \in D} \left(\left| Loss(f(x_i), y_i) - Loss(\hat{f}(x_i), y_i) \right| + \left| Loss(\hat{f}(x_i), y_i) - Loss(\hat{f}(x_i), y_{cpl,i}) \right| \right) \quad (5) \end{aligned}$$

Definition Denotes the j^{th} output of \hat{f}_{cpl} as \hat{f}_{cpl}^j . Label mapping function g converts NTK's predictions about CPL classes, $\hat{f}_{cpl}(x_i)$, into predictions about true classes, $\hat{f}_{y_{map}}(x_i)$, based on dominant labels within corresponding CPL classes as shown in eq. 6, where D_{dom} is a set of index k , where j is the dominant true label classes within CPL class, $y_{cpl,k}$.

$$\hat{f}_{y_{map}}^j(x_i) = \sum_{k \in D_{dom}} \hat{f}_{cpl}^k(x_i) \quad (6)$$

Proposition If the true labels of labeled samples are the dominant labels in their corresponding CPL clusters, $\hat{f}_y(x_i) = g(\hat{f}_{cpl}(x_i))$. We defer the proof to appendix 6.1.

$$error_{CPL} = P_{nff} + P_{fnf} \quad (7)$$

As mentioned in sec. 3.2, we use 0-1 loss to calculate empirical risk. We can expand $error_{CPL}$ as eq. 7, where we denote the probability that the NTK prediction agrees with the y but not with y_{cpl} as P_{fnf} , and the probability that the NTK prediction does not agree with y but agrees with y_{cpl} as P_{nff} . According to the proposition, we argue $argmax_{\hat{f}_y}(x_i)$ is most likely equal to $g(argmax_{\hat{f}_{cpl}}(x_i))$. P_{fnf} refers to the case where different CPL classes correspond to the same true label class, i.e., over-clustering. P_{nff} means that the true label of a sample is different from the dominant true label within its CPL class, i.e., the CPL class includes samples from different true label classes, which is called impurity. Detailed explanations and empirical evidence can be found in appendix 6.1.

3.4 Cluster Pseudo-Labels

As shown by eq. 7, the effect of CPL on the approximation error comes from the purity of the clusters and over-clustering. To improve clustering purity, we take two approaches: (1) clustering on the active learning feature, i.e., the output of the penultimate layer of the classifier, and (2) increasing the number of clusters. However, increasing the number of clusters may cause the labeled samples not to cover all classes of the CPL (under-coverage) and also increase the over-clustering error. For example, a group of samples with the same true label is clustered into K different classes. Even though NTK incorrectly predicts some samples as other CPL classes, their true empirical risk is zero.

To improve the under-coverage, we set the number of clusters to half of the total number of labels, i.e., each cluster includes two labeled samples on average. To improve the over-clustering, we manually set the maximum number of clusters and design a clustering-splitting approach instead of directly increasing the number of clusters. It splits the low-purity clusters and keeps the high-purity ones to reduce the extra over-clustering errors within samples located in the high-purity clusters. Specifically, we use the prediction of the neural network in each round of active learning to estimate the number of confusing samples within each cluster, i.e., the number of samples from classes that are different from the dominant class. The clusters that contain the largest number of confusing samples are split sequentially until a predefined number of clusters is reached. The cluster splitting algorithm is shown in Alg. 2, where we adopt the constrained K-Means [37] to improve the clusters from labeled sample constraints.

Algorithm 2 CPL generation

Input: active learning feature f_{al} , model predictions Y_{pre} , initial cluster number C_0 , cluster number C_{max} , labeled set L
Output: CPL Y_{cpl}
 $Clu_{1,\dots,C_0} \leftarrow$ Constrained K-means(f_{al}, L, C_0)
for $itr = 1$ **to** $(C_{max} - C_0)$ **do**
 $i' = argmax_i$ number of Confusing samples(Clu_i, Y_{pre})
 $f_{al,i'} \leftarrow f_{al}$ of samples within $Clu_{i'}$
 $Clu_{i',C_0+1} \leftarrow$ K-means($f_{al,i'}, 2$)
 $C_0 \leftarrow C_0 + 1$
end for
 $Y_{cpl} \leftarrow Clu_{1,\dots,C_{max}}$

4 Experiment Results

Our approach is validated on five datasets with various qualities of self-supervised features. Datasets with good self-supervised features, such as CIFAR-10 [21], CIFAR-100 [21], and ImageNet-100 (a subset of ImageNet [11], following splitting in [36]), are included. SVHN [29] with poor self-supervised features is also included. Additionally, we consider practical scenarios where the total number of samples in the trainset is insufficient to support effective self-supervised training, such as Oxford-IIIT Pet dataset [30]. In this case, we evaluated the effectiveness of our method based on the model pre-trained on ImageNet [11].

Baseline We compare our proposed method with representative active learning strategies: (1) Random, (2) Entropy (uncertainty sampling, maximum entropy of output) [22], (3) Coreset (diversity active learning strategy, greedy solution of minimum coverage radius) [32], (4) BADGE (combination of uncertainty and diversity, kmeans++ sampling on grad embedding) [3], where the scalable version [10, 12], badge partition, is used in ImageNet-100, CIFAR-100 and Oxford-IIIT Pet because the huge dimension of grad embedding (5) Typiclust (designed for low-budget case) [15], (6) Lookahead (maximum output change based on NTK) [26].

Table 1: Comparison of accuracy of different active learning strategies on CIFAR-10. All results are averages over 5 runs. The best results are shown in red and the second-best results are shown in blue.

# Labels	Random	Entropy	Coreset(self)	BADGE	TypiClust	LookAhead	NTKCPL(self)	NTKCPL(al)
20	41.80±3.82	38.58±2.86	20.08±2.75	39.85±3.91	46.38±1.61	40.93±4.04	54.31±3.74	52.67±3.70
40	57.52±3.34	51.10±4.21	36.67±6.29	54.99±3.43	66.18±2.45	58.55±2.71	68.60±2.50	63.55±2.89
60	65.88±3.07	64.46±3.42	46.39±7.41	65.23±1.40	72.93±1.77	66.96±2.90	75.09±1.69	72.22±2.11
80	69.35±3.31	70.49±3.05	58.96±6.15	70.76±1.86	76.98±1.04	72.71±1.94	78.51±1.61	75.32±0.92
100	74.11±1.16	74.34±1.92	62.64±5.07	75.40±0.99	78.24±1.28	75.97±2.04	80.30±1.17	78.45±1.19
200	80.90±0.90	79.86±1.77	76.93±3.56	82.20±1.14	83.16±0.61	81.89±1.31	83.77±1.04	81.87±1.02
300	82.80±0.93	81.43±2.23	82.64±1.42	84.53±0.46	84.16±0.25	83.29±0.89	85.00±0.54	83.78±1.05
400	84.04±0.49	83.37±1.31	84.56±1.15	84.75±0.40	85.13±0.27	84.59±0.59	85.64±0.38	84.73±0.85
500	84.97±0.78	84.24±0.89	85.23±0.59	85.57±0.51	85.37±0.15	85.31±0.12	85.72±0.22	85.48±0.65
1000	86.26±0.38	84.94±0.48	86.75±0.36	86.06±0.31	86.07±0.14	85.69±0.47	86.83±0.33	87.15±0.57
1500	86.95±0.27	85.85±0.39	87.03±0.13	87.05±0.36	86.37±0.11	86.82±0.23	87.18±0.41	87.58±0.29
2000	87.30±0.37	86.92±0.15	87.34±0.27	87.31±0.47	86.55±0.21	87.16±0.19	87.34±0.41	87.87±0.39

Implementation Our method focuses on the low-budget regime, we followed the training method in [24], freezing weights of backbone initialized with self-supervised learning and then training a MLP as the classifier. The hyperparameters for training are set following [15] and can be found in appendix 6.3. For the self-supervised model, we adopt simsiam [9] for CIFAR-10, CIFAR-100 and SVHN and BYOL [14] for ImageNet-100 and Oxford-IIIT Pet. Resnet-18 [17] is used in CIFAR-10 and SVHN, WRN28-8 [44] is used in CIFAR-100 and Resnet-50 [17] is used in ImageNet-100 and Oxford-IIIT Pet.

The number of clusters in our method is set according to three rules, in the initial selection, it is set to the number of query samples, after that it is set to half of the query samples until the number of clusters reaches the maximum number of clusters. For CIFAR-10, CIFAR-100, ImageNet-100, SVHN, and Oxford-IIIT Pet, the maximum number of clusters is 100, 500, 300, 100, and 150, respectively. We followed [26] to sample a subset of the unlabeled set as the candidate set to select samples and estimate coverage. The candidate set includes 10,000 samples.

For the query step, most of the experiments (those on CIFAR-100, SVHN and Oxford-IIIT Pet) following the active learning literature by drawing a fixed number of samples from the unlabeled dataset to the oracle. Specifically, 500 for CIFAR-100, 20 for SVHN, and 40 for Oxford-IIIT Pet. We empirically found that fixed active learning query steps lead to much faster growth of classifier accuracy in the early stages of active learning (the amount of labels is about 10 times than the number of class) than in the later stages, so it is difficult to clearly observe the differences between different active learning strategies. For this reason, we empirically set varying query steps in our experiments with CIFAR-10 and ImageNet-100. Smaller query steps were used in the early stage of active learning and switched to larger query steps in the later stage. Specifically, for CIFAR-10, 20 samples are queried before 100 labels are available, 100 samples are queried before 500 labels and 500 labels are queried before 2000 labels. For ImageNet-100, 200 samples are selected before 1000 labels are available and 500 samples are queried before 2000 labels.

4.1 Main Results

All experiments were run 5 times and the avg. and std. are reported. Considering that the experiments are conducted for the scenario with a low annotation budget, it is not practical to construct a validation set to select the best checkpoints (the benefits of constructing a validation set are much less than using these labeled samples as training samples). Therefore, we report the final checkpoint accuracy, not the accuracy of the checkpoints determined by the validation set. The results are shown in fig. 2 and table 1. The detailed results are in appendix 6.5.

NTKCPL outperforms SOTA. As shown in table 1, fig. 2. In most cases, our proposed method outperforms the baseline methods. For the few cases with only a small number of labels, our method shows comparable performance with the low-budget strategy, TypiClust, such as in CIFAR-100 with 500 and 1000 labeled samples, and Oxford-IIIT Pet with 80 and 100 labeled samples.

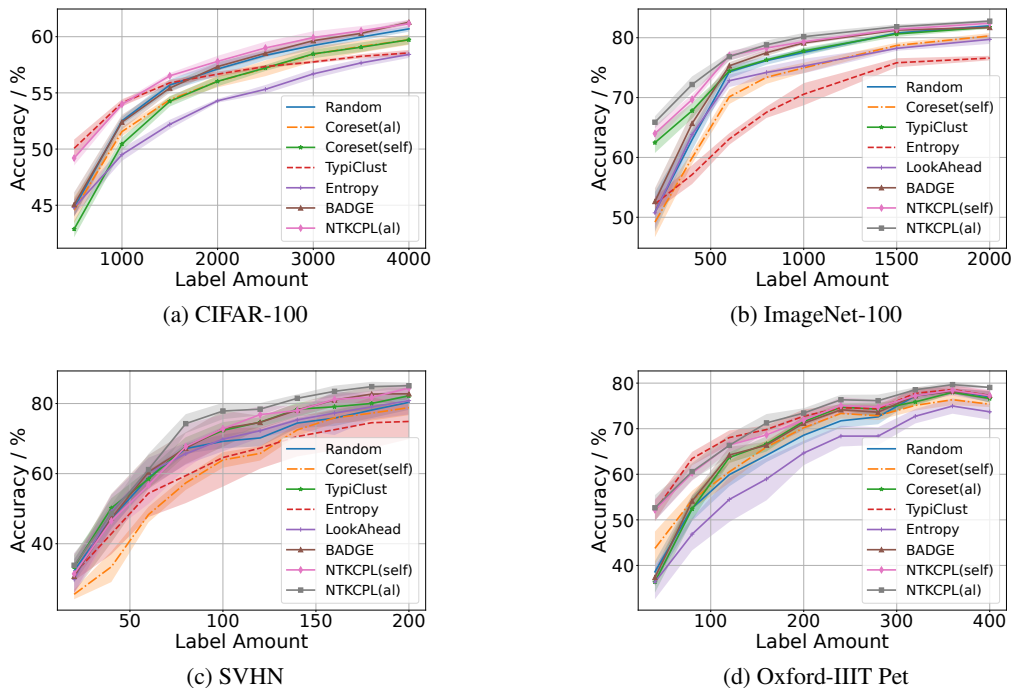


Figure 2: Performance of different active learning strategies. The shaded area represents std.

NTKCPL still shows good performance when the self-supervised features do not correspond well to the label classes. Since the loss of self-supervised training is different from that of image classification, self-supervised features do not always correspond well with label classes. In SVHN dataset, self-supervised features of different classes are mixed together because the images include some irrelevant digits on both sides of the digit of interest [29]. Our method is similar to other baseline strategies at the beginning of active learning, but it shows better results than baselines after several active learning rounds as shown in fig. 2c.

Another common scenario is the lack of sufficient samples to support effective self-supervised training. To evaluate in this context, we choose the Oxford-IIIT Pet dataset with the self-supervised model trained on ImageNet. The result is shown in fig. 2d. Our method has similar accuracy in the first three rounds as the TypiClust and outperforms all baseline methods afterward.

NTKCPL has a wider effective budget range than SOTA.

Active learning based on self-supervised models exhibits an intensified phase transition phenomenon. We plot the active learning gain of our method and baselines on different datasets in fig. 3. The average accuracy of our method, NTKCPL(al), outperforms the random baseline at all quantities of labels. In contrast, both the typical high-budget strategy, BADGE, and low-budget strategy, TypiClust, appear to be worse than the random baseline over a range of annotation quantities. We show the effective budget range of our method, NTKCPL, as well as the typical high-budget strategy, BADGE, and the typical low-budget strategy, TypiClust, across all experiments in table 2. The effective budget ratio refers to the proportion of the effective annotation quantity to the total annotation quantity, where the effective annotation quantity refers to the number of annotations at which active learning accuracy exceeds the random baseline (avg. + std.).

Table 2: Comparison of the effective budget ratio of different active learning strategies.

	Effective Budget Ratio
TypiClust	40.8%
BADGE	42.0%
NTKCPL(al)	92.7%

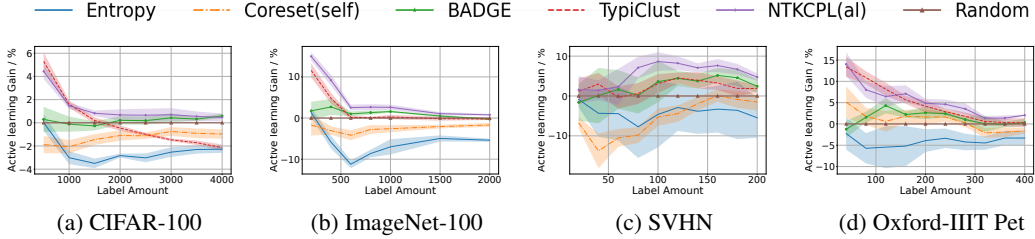


Figure 3: Active learning gain of different active learning strategies.

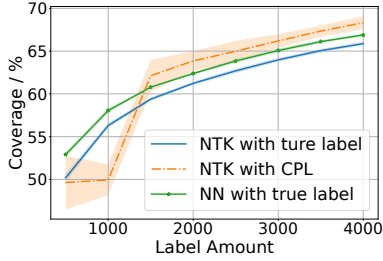


Figure 4: Coverage estimation on CIFAR-100.

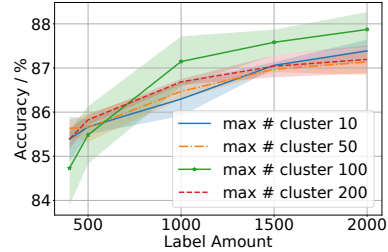


Figure 5: Effect of the maximum number of clusters on active learning performance on CIFAR-10.

4.2 Ablation Study

In this section, we evaluate the coverage estimation of our method and the effect of the maximum cluster number on NTKCPL. Also, we compare the effect of generating CPL on self-supervised features as well as on the active learning feature on the performance of NTKCPL.

Coverage Estimation We conducted experiments on CIFAR-100, where the coverage indicates the proportion of samples that are correctly predicted. The estimated coverage of NTK with true label and with CPL is shown in fig. 4. Our method approximates the true coverage well for most cases.

Effect of the Maximum Number of CPL The ablation experiments are conducted on CIFAR-10. We plot the accuracy when the number of annotations selected by active learning is greater than 400 as shown in fig. 5. In this range, the number of classes of CPL is fixed at 10, 50, 100, and 200, respectively. The experimental results support our analysis in sec. 3.4 that too many or too few clusters will increase the approximation error, which affects the performance of active learning.

Effect of self-supervised feature-based and active learning feature-based clustering-pseudo-labels on NTKCPL. We denote NTKCPL based on active learning features as NTKCPL(al) and NTKCPL based on self-supervised learning feature as NTKCPL(self). The results are shown in table 1 and fig. 2. From these experiments, we found that clustering on active learning features yields better results except for the case where the number of annotations is very small. Also, NTKCPL(self) is better than NTKCPL(al) in a wide range of annotation quantities (no more than 500), when self-supervised features are good such as experiment in the CIFAR-10.

5 Conclusion

We study the active learning problem when training on top of a self-supervised model. In this case, an intensified phase transition is observed and it influences the application of active learning. We propose NTKCPL that approximates empirical risk on the whole pool more directly. We also analyze the approximation error and design a CPL generation method based on the analysis to reduce the approximation error. Our method outperforms SOTA in most cases and has a wider effective budget range. The comprehensive experiments show that our method can work well on self-supervised features with different qualities.

Our approach is limited to the fixed training approach, i.e., training the classifier on top of a frozen self-supervised training encoder, which is restricted to the low-budget scenario because the fine-tuning training approach provides higher accuracy in the high-budget case. Therefore, (1) how to accurately approximate the fine-tuning model initialized with self-supervised weights using NTK and (2) whether the samples selected by our current method have good transferability for the fine-tuning would be interesting future directions.

References

- [1] Inigo Alonso, Matan Yuval, Gal Eyal, Tali Treibitz, and Ana C Murillo. Coralseg: Learning coral segmentation from sparse annotations. *Journal of Field Robotics*, 36(8):1456–1477, 2019.
- [2] Sanjeev Arora, Simon S Du, Wei Hu, Zhiyuan Li, Russ R Salakhutdinov, and Ruosong Wang. On exact computation with an infinitely wide neural net. *Advances in neural information processing systems*, 32, 2019.
- [3] Jordan T. Ash, Chicheng Zhang, Akshay Krishnamurthy, John Langford, and Alekh Agarwal. Deep batch active learning by diverse, uncertain gradient lower bounds. In *International Conference on Learning Representations*, 2020.
- [4] Javad Zolfaghari Bengar, Joost van de Weijer, Bartłomiej Twardowski, and Bogdan Raducanu. Reducing label effort: Self-supervised meets active learning. In *Proceedings of the IEEE/CVF International Conference on Computer Vision*, pages 1631–1639, 2021.
- [5] Zalán Borsos, Marco Tagliasacchi, and Andreas Krause. Semi-supervised batch active learning via bilevel optimization. In *ICASSP 2021-2021 IEEE International Conference on Acoustics, Speech and Signal Processing (ICASSP)*, pages 3495–3499. IEEE, 2021.
- [6] Yao-Chun Chan, Mingchen Li, and Samet Oymak. On the marginal benefit of active learning: Does self-supervision eat its cake? In *ICASSP 2021-2021 IEEE International Conference on Acoustics, Speech and Signal Processing (ICASSP)*, pages 3455–3459. IEEE, 2021.
- [7] Ting Chen, Simon Kornblith, Mohammad Norouzi, and Geoffrey Hinton. A simple framework for contrastive learning of visual representations. In *International conference on machine learning*, pages 1597–1607. PMLR, 2020.
- [8] Ting Chen, Simon Kornblith, Kevin Swersky, Mohammad Norouzi, and Geoffrey E Hinton. Big self-supervised models are strong semi-supervised learners. *Advances in neural information processing systems*, 33:22243–22255, 2020.
- [9] Xinlei Chen and Kaiming He. Exploring simple siamese representation learning. In *Proceedings of the IEEE/CVF Conference on Computer Vision and Pattern Recognition*, pages 15750–15758, 2021.
- [10] Gui Citovsky, Giulia DeSalvo, Claudio Gentile, Lazaros Karydas, Anand Rajagopalan, Afshin Ros-tamizadeh, and Sanjiv Kumar. Batch active learning at scale. *Advances in Neural Information Processing Systems*, 34:11933–11944, 2021.
- [11] Jia Deng, Wei Dong, Richard Socher, Li-Jia Li, Kai Li, and Li Fei-Fei. Imagenet: A large-scale hierarchical image database. In *2009 IEEE conference on computer vision and pattern recognition*, pages 248–255. Ieee, 2009.
- [12] Zeyad Ali Sami Emam, Hong-Min Chu, Ping-Yeh Chiang, Wojciech Czaja, Richard Leapman, Micah Goldblum, and Tom Goldstein. Active learning at the imagenet scale. *arXiv preprint arXiv:2111.12880*, 2021.
- [13] Yarín Gal, Riashat Islam, and Zoubin Ghahramani. Deep bayesian active learning with image data. In *International Conference on Machine Learning*, pages 1183–1192. PMLR, 2017.
- [14] Jean-Bastien Grill, Florian Strub, Florent Altché, Corentin Tallec, Pierre Richemond, Elena Buchatskaya, Carl Doersch, Bernardo Avila Pires, Zhaohan Guo, Mohammad Gheshlaghi Azar, et al. Bootstrap your own latent—a new approach to self-supervised learning. *Advances in Neural Information Processing Systems*, 33:21271–21284, 2020.
- [15] Guy Hacohen, Avihu Dekel, and Daphna Weinshall. Active learning on a budget: Opposite strategies suit high and low budgets. In *International Conference on Machine Learning*, pages 8175–8195. PMLR, 2022.
- [16] Guy Hacohen and Daphna Weinshall. Misal: Active learning for every budget. 2023.
- [17] Kaiming He, Xiangyu Zhang, Shaoqing Ren, and Jian Sun. Deep residual learning for image recognition. In *Proceedings of the IEEE conference on computer vision and pattern recognition*, pages 770–778, 2016.
- [18] Arthur Jacot, Franck Gabriel, and Clément Hongler. Neural tangent kernel: Convergence and generalization in neural networks. *Advances in neural information processing systems*, 31, 2018.

- [19] Andreas Kirsch, Joost Van Amersfoort, and Yarin Gal. Batchbald: Efficient and diverse batch acquisition for deep bayesian active learning. *Advances in neural information processing systems*, 32, 2019.
- [20] Seo Taek Kong, Soomin Jeon, Dongbin Na, Jaewon Lee, Hong-Seok Lee, and Kyu-Hwan Jung. A neural pre-conditioning active learning algorithm to reduce label complexity. *Advances in Neural Information Processing Systems*, 35:32842–32853, 2022.
- [21] Alex Krizhevsky, Geoffrey Hinton, et al. Learning multiple layers of features from tiny images. 2009.
- [22] David D Lewis and Jason Catlett. Heterogeneous uncertainty sampling for supervised learning. In *Machine learning proceedings 1994*, pages 148–156. Elsevier, 1994.
- [23] Ze Liu, Yutong Lin, Yue Cao, Han Hu, Yixuan Wei, Zheng Zhang, Stephen Lin, and Baining Guo. Swin transformer: Hierarchical vision transformer using shifted windows. In *Proceedings of the IEEE/CVF International Conference on Computer Vision*, pages 10012–10022, 2021.
- [24] Rafid Mahmood, Sanja Fidler, and Marc T Law. Low-budget active learning via wasserstein distance: An integer programming approach. In *International Conference on Learning Representations*, 2022.
- [25] Sudhanshu Mittal, Maxim Tatarchenko, Özgün Çiçek, and Thomas Brox. Parting with illusions about deep active learning. *arXiv preprint arXiv:1912.05361*, 2019.
- [26] Mohamad Amin Mohamadi, Wonho Bae, and Danica J Sutherland. Making look-ahead active learning strategies feasible with neural tangent kernels. In *Advances in Neural Information Processing Systems*, 2022.
- [27] Mohamad Amin Mohamadi and Danica J Sutherland. A fast, well-founded approximation to the empirical neural tangent kernel. *arXiv preprint arXiv:2206.12543*, 2022.
- [28] Prateek Munjal, Nasir Hayat, Munawar Hayat, Jamshid Sourati, and Shadab Khan. Towards robust and reproducible active learning using neural networks. In *Proceedings of the IEEE/CVF Conference on Computer Vision and Pattern Recognition*, pages 223–232, 2022.
- [29] Yuval Netzer, Tao Wang, Adam Coates, Alessandro Bissacco, Bo Wu, and Andrew Y Ng. Reading digits in natural images with unsupervised feature learning. 2011.
- [30] Omkar M Parkhi, Andrea Vedaldi, Andrew Zisserman, and CV Jawahar. Cats and dogs. In *2012 IEEE conference on computer vision and pattern recognition*, pages 3498–3505. IEEE, 2012.
- [31] Kossar Pourahmadi, Parsa Nooralinejad, and Hamed Pirsiavash. A simple baseline for low-budget active learning. *UMBC Student Collection*, 2022.
- [32] Ozan Sener and Silvio Savarese. Active learning for convolutional neural networks: A core-set approach. In *International Conference on Learning Representations*, 2018.
- [33] Changjian Shui, Fan Zhou, Christian Gagné, and Boyu Wang. Deep active learning: Unified and principled method for query and training. In *International Conference on Artificial Intelligence and Statistics*, pages 1308–1318. PMLR, 2020.
- [34] Samarth Sinha, Sayna Ebrahimi, and Trevor Darrell. Variational adversarial active learning. In *Proceedings of the IEEE/CVF International Conference on Computer Vision*, pages 5972–5981, 2019.
- [35] Toan Tran, Thanh-Toan Do, Ian Reid, and Gustavo Carneiro. Bayesian generative active deep learning. In *International Conference on Machine Learning*, pages 6295–6304. PMLR, 2019.
- [36] Wouter Van Gansbeke, Simon Vandenhende, Stamatios Georgoulis, Marc Proesmans, and Luc Van Gool. Scan: Learning to classify images without labels. In *Computer Vision—ECCV 2020: 16th European Conference, Glasgow, UK, August 23–28, 2020, Proceedings, Part X*, pages 268–285. Springer, 2020.
- [37] Kiri Wagstaff, Claire Cardie, Seth Rogers, Stefan Schrödl, et al. Constrained k-means clustering with background knowledge. In *Icml*, volume 1, pages 577–584, 2001.
- [38] Haonan Wang, Wei Huang, Ziwei Wu, Hanghang Tong, Andrew J Margenot, and Jingrui He. Deep active learning by leveraging training dynamics. *Advances in Neural Information Processing Systems*, 35:25171–25184, 2022.
- [39] Ziting Wen, Oscar Pizarro, and Stefan Williams. Active self-semi-supervised learning for few labeled samples fast training. *arXiv e-prints*, pages arXiv–2203, 2022.
- [40] Yichen Xie, Han Lu, Junchi Yan, Xiaokang Yang, Masayoshi Tomizuka, and Wei Zhan. Active finetuning: Exploiting annotation budget in the pretraining-finetuning paradigm. *arXiv preprint arXiv:2303.14382*, 2023.
- [41] Lin Yang, Yizhe Zhang, Jianxu Chen, Siyuan Zhang, and Danny Z Chen. Suggestive annotation: A deep active learning framework for biomedical image segmentation. In *International conference on medical image computing and computer-assisted intervention*, pages 399–407. Springer, 2017.
- [42] Ofer Yehuda, Avihu Dekel, Guy Hacohen, and Daphna Weinshall. Active learning through a covering lens. In *Advances in Neural Information Processing Systems*, 2022.

- [43] Donggeun Yoo and In So Kweon. Learning loss for active learning. In *Proceedings of the IEEE/CVF conference on computer vision and pattern recognition*, pages 93–102, 2019.
- [44] Sergey Zagoruyko and Nikos Komodakis. Wide residual networks. In *British Machine Vision Conference 2016*. British Machine Vision Association, 2016.
- [45] Wenqiao Zhang, Lei Zhu, James Hallinan, Shengyu Zhang, Andrew Makmur, Qingpeng Cai, and Beng Chin Ooi. Boostmis: Boosting medical image semi-supervised learning with adaptive pseudo labeling and informative active annotation. In *Proceedings of the IEEE/CVF Conference on Computer Vision and Pattern Recognition*, pages 20666–20676, 2022.

6 Appendix

6.1 Proof of Proposition

When the training set is \mathcal{X} , the prediction of NTK for the test sample x , $\hat{f}(x)$, is as in eq. 8, where \mathcal{Y} denotes labels of training samples with one-hot form and we denote $\mathcal{K}(x, \mathcal{X})\mathcal{K}(\mathcal{X}, \mathcal{X})^{-1}$ as weight matrix W . The difference between NTK predictions with true labels, $\hat{f}_y(x)$, and predictions with CPL transformed to true label classes through a label mapping function g , $g(\hat{f}_{cpl}(x))$, as shown in eq. 9. We write the product of the row vector W and the labels as the element-wise multiplication, where w_i represents the i^{th} element of W . When true labels of labeled samples are the dominant labels in their corresponding CPL clusters, $y_i = g(y_{cpl,i})$ and the result of the eq. 9 is zero, i.e., $\hat{f}_y(x) = g(\hat{f}_{cpl}(x))$.

$$\begin{aligned}\hat{f}(x) &= \hat{f}_0(x) + \mathcal{K}(x, \mathcal{X})\mathcal{K}(\mathcal{X}, \mathcal{X})^{-1}(\mathcal{Y} - f_0(\mathcal{X})) \\ &= \hat{f}_0(x) + W\hat{f}_0(x) - W\mathcal{Y}\end{aligned}\tag{8}$$

$$\begin{aligned}\hat{f}_y(x) - g(\hat{f}_{cpl}(x)) &= W\mathcal{Y} - g(W\mathcal{Y}_{cpl}) \\ &= \sum_{i \in D_C} (w_i y_i) - \sum_{i \in D_C} (w_i g(y_{cpl,i})) \\ &= \sum_{i \in D_C} w_i (y_i - g(y_{cpl,i}))\end{aligned}\tag{9}$$

Empirical evidence of assumption Based on proposition, $\hat{f}_y(x_i) = g(\hat{f}_{cpl}(x_i))$, we argue $\text{argmax}_y \hat{f}_y(x_i)$ is most likely equal to $g(\text{argmax}_y \hat{f}_{cpl}(x_i))$. We validate this claim on the CIFAR-10 and CIFAR-100 datasets. The validity of this claim at different numbers of annotations is shown in fig. 6. This claim is valid in most cases, especially when the dataset has few classes.

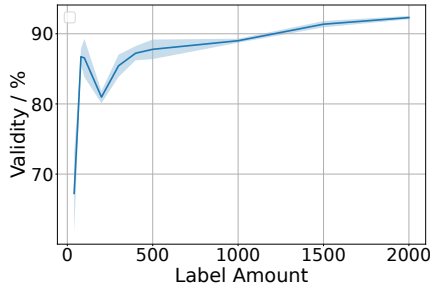
Explanation of impurity error and over-clustering error As analyzed in sec.3.3, the approximation error consists of P_{fnf} and P_{nff} . The P_{fnf} denotes the NTK prediction agrees with y but does not agree with y_{cpl} . From our claim, it can be deduced that the true label class y_i corresponds to at least two different CPL classes: $y_{cpl,i}$ and $\text{argmax}_y \hat{f}_{cpl}(x_i)$, i.e., over-clustering.

The P_{nff} denotes the NTK prediction does not agree with y but agrees with y_{cpl} . Based on our claim, $\text{argmax}_y \hat{f}_y(x_i)$ would be the dominant class within the CPL. But it is different from the true label, y_i , i.e., y_i is not the dominant class within this CPL cluster. So, this CPL cluster includes the impure sample.

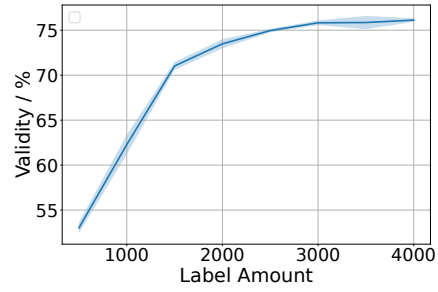
Empirical evidence of impurity error and over-clustering error To validate the analysis of over-clustering error and impurity error, we conducted experiments on the CIFAR-10 and CIFAR-100 datasets. Specifically, we examined the ratios of impure samples within CPL in the P_{nff} term and the ratios of over-clustering in the P_{fnf} term. The results are shown in fig. 7 and fig. 8. The experimental results show that impurity and over-clustering explain most of the approximation errors.

6.2 Dataset Description

CIFAR-10 and CIFAR-100 datasets both consist of 50,000 training samples and 10,000 testing samples, with a resolution of 32x32. CIFAR-10 is composed of 10 classes, while CIFAR-100 consists of 100 classes. Similarly, SVHN dataset also contains 10 classes, with 73,257 training samples and 26,032 testing samples. Its resolution is 32x32. ImageNet-100 is a subset of the ImageNet dataset, comprising 100 classes, with 128,545 training samples and 5,000 testing samples. Oxford-IIIT Pet dataset includes 37 classes, with 3,680 training samples

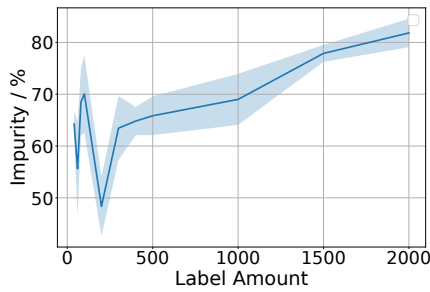


(a) CIFAR-10

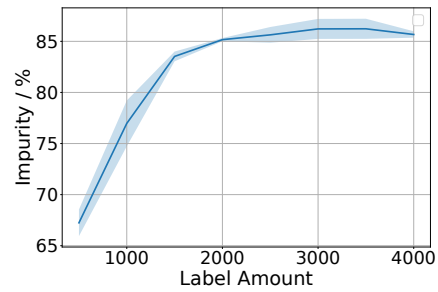


(b) CIFAR-100

Figure 6: The validity of the claim ($\operatorname{argmax}_{\hat{f}_y}(x_i) = g(\operatorname{argmax}_{\hat{f}_{cpl}}(x_i))$) at different numbers of annotations. The shaded area represents std.

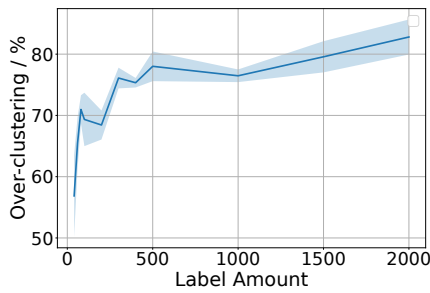


(a) CIFAR-10

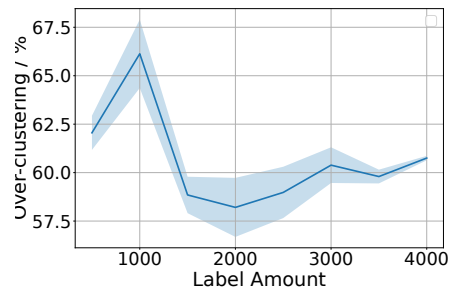


(b) CIFAR-100

Figure 7: Proportion of approximation error caused by impure samples within CPL to the $P_{n,ff}$ term. The shaded area represents std.



(a) CIFAR-10



(b) CIFAR-100

Figure 8: Proportion of approximation error caused by over-clustering of CPL to the P_{fnf} term. The shaded area represents std.

and 3,669 testing samples. For both ImageNet-100 and Oxford-IIIT Pet dataset, all samples were resized to a resolution of 224x224 following the method described in [14].

6.3 Hyperparameters of Training

Classifier is a 2-layer MLP with the architecture: Linear + BatchNorm + ReLU + Linear. The dimension of the output of the first linear layer is shown in table 3. Total number of training epochs is 100. Data augmentation includes random crops and horizontal flips. The remaining hyperparameters are shown in table 3.

Table 3: Hyperparameters

Dataset	Backbone	Classifier	Learning Rate	Momentum	Weight Decay	Batch Size
CIFAR-10	Resnt18	MLP64	0.3	0.9	0.0003	100
CIFAR-100	WRN-28-8	MLP512	0.3	0.9	0.0003	100
ImageNet-100	Resnet50	MLP4096	0.1	0.9	0	512
SVHN	Resnt18	MLP512	0.3	0.9	0.0003	100
Oxford-IIIT Pet	Resnet50	MLP512	0.1	0.9	0	128

6.4 Computation time

We compare the computation time of our method with that of LookAhead [26] (an active learning method based on NTK) as shown in fig. 9. Our method demonstrates a comparable sample selection time to LookAhead. When the dataset with few classes, our method takes slightly longer than LookAhead. Conversely, when the dataset with many classes, our method takes slightly less time than LookAhead.

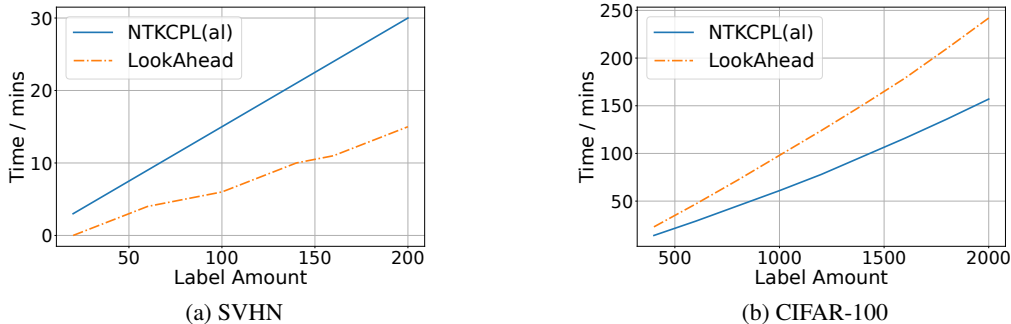


Figure 9: Comparison of cumulative sample selection time on single RTX 3090 GPU.

6.5 Experiment Results

The results of the experiment are shown in table 4, table 5, table 6 and table 7, where we report the average accuracy and std. over 5 runs.

Table 4: Comparison of accuracy of different active learning strategies on CIFAR-100 with budget step size 500. All results are averages over 5 runs. The best results are shown in red and the second-best results are shown in blue.

# Labels	Random	Entropy	Coresset(self)	Coresset(al)	BADGE	TypiClust	NTKCPL(al)
500	44.76±0.77	44.79±0.71	42.88±0.73	44.56±1.16	45.06±1.08	50.06±0.79	49.20±0.66
1000	52.51±0.36	49.50±0.56	50.44±0.58	51.55±0.41	52.40±0.66	54.12±0.31	53.99±0.27
1500	55.70±0.51	52.19±0.41	54.25±0.47	54.38±0.29	55.43±0.40	55.89±0.27	56.52±0.24
2000	57.12±0.62	54.30±0.17	56.03±0.45	56.02±0.54	57.34±0.36	56.67±0.23	57.80±0.49
2500	58.34±0.42	55.32±0.38	57.22±0.27	57.19±0.70	58.53±0.35	57.35±0.13	59.00±0.56
3000	59.22±0.38	56.69±0.42	58.47±0.38	58.44±0.68	59.64±0.39	57.75±0.12	59.92±0.57
3500	59.97±0.30	57.67±0.36	59.06±0.42	59.13±0.54	60.29±0.16	58.25±0.20	60.53±0.42
4000	60.70±0.25	58.42±0.32	59.73±0.40	59.73±0.46	61.29±0.20	58.55±0.27	61.16±0.34

Table 5: Comparison of accuracy of different active learning strategies on ImageNet-100. All results are averages over 5 runs. The best results are shown in red and the second-best results are shown in blue.

# Labels	Random	Entropy	Coreset(self)	BADGE	TypiClust	LookAhead	NTKCPL(self)	NTKCPL(al)
200	50.89±3.33	52.21±1.17	49.19±2.54	52.64±2.21	62.47±1.73	50.75±2.71	63.98±1.39	65.88±1.00
400	62.98±1.81	57.13±1.59	59.94±1.03	65.68±1.95	67.81±1.31	63.82±0.56	69.69±0.78	72.18±1.36
600	74.30±1.09	63.09±0.97	70.13±1.21	75.31±0.60	74.45±0.45	72.82±1.06	77.03±0.77	76.84±0.72
800	76.17±0.68	67.55±0.95	73.39±1.09	77.50±0.53	76.30±0.17	74.20±1.00	78.28±0.58	78.81±0.71
1000	77.56±0.59	70.56±1.85	74.96±0.87	79.13±0.27	77.80±0.55	75.27±1.22	79.34±0.44	80.17±0.64
1500	80.78±0.16	75.82±0.76	78.71±0.45	81.28±0.23	80.63±0.49	78.23±0.41	81.41±0.31	81.84±0.40
2000	81.98±0.28	76.60±0.38	80.30±0.47	81.71±0.27	81.76±0.25	79.73±0.76	82.42±0.56	82.77±0.21

Table 6: Comparison of accuracy of different active learning strategies on SVHN. All results are averages over 5 runs. The best results are shown in red and the second-best results are shown in blue.

# Labels	Random	Entropy	Coreset(self)	BADGE	TypiClust	LookAhead	NTKCPL(self)	NTKCPL(al)
20	32.30±3.44	31.41±2.00	25.57±1.42	30.70±4.61	33.42±3.28	29.88±3.86	31.40±5.76	33.87±3.42
40	47.19±3.06	42.84±5.89	33.41±4.35	47.28±6.95	50.18±2.79	49.27±4.70	46.51±3.26	48.63±2.49
60	58.84±1.72	54.40±6.78	48.32±2.23	60.48±4.86	58.47±2.79	60.34±4.21	56.73±5.38	61.16±4.52
80	67.15±1.46	59.42±7.84	57.33±1.99	67.27±4.54	67.77±2.63	65.66±3.13	67.73±6.35	74.26±2.71
100	69.22±1.97	64.59±8.29	63.91±2.22	72.83±5.21	72.33±2.37	69.85±3.48	72.80±4.11	77.87±2.33
120	70.18±2.40	67.29±5.88	65.77±2.04	74.61±1.90	74.68±1.40	72.24±2.04	76.85±2.34	78.39±1.75
140	74.43±1.44	70.60±5.67	72.49±1.69	78.16±1.89	78.38±2.06	75.33±2.76	78.01±1.40	81.50±1.13
160	75.84±2.26	72.54±5.88	75.93±1.56	81.00±1.84	79.08±1.71	77.28±6.27	81.20±1.40	83.48±1.64
180	78.13±2.26	74.53±7.23	77.26±2.14	82.70±2.10	80.03±1.97	79.05±3.51	81.77±1.83	84.83±1.36
200	80.35±2.16	74.88±5.02	78.83±2.15	82.78±1.72	82.21±0.88	80.83±3.95	84.40±1.40	85.08±0.91

Table 7: Comparison of accuracy of different active learning strategies on Oxford-IIIT Pet. All results are averages over 5 runs. The best results are shown in red and the second-best results are shown in blue.

# Labels	Random	Entropy	Coreset(self)	Coreset(al)	BADGE	TypiClust	NTKCPL(self)	NTKCPL(al)
40	38.60±2.33	36.35±3.78	43.73±3.70	36.40±2.39	37.37±1.95	51.99±2.34	52.19±2.40	52.64±2.79
80	52.57±2.82	46.86±3.56	54.35±2.03	52.41±2.55	54.13±1.31	63.45±1.47	60.27±1.71	60.59±1.86
120	59.91±2.56	54.47±4.94	60.54±2.43	63.69±1.16	64.21±1.81	68.05±1.57	66.42±1.36	66.35±2.44
160	64.16±1.49	58.96±4.69	65.97±1.54	66.66±1.66	66.39±0.74	69.82±0.91	68.63±1.31	71.27±1.95
200	68.57±1.86	64.66±2.67	70.21±1.71	71.57±0.98	71.20±1.49	72.74±1.48	71.92±1.43	73.43±1.06
240	71.73±1.47	68.37±2.29	73.35±1.12	74.73±0.84	74.15±0.85	74.60±0.74	75.07±1.84	76.35±1.09
280	72.60±1.63	68.37±1.94	72.84±0.95	74.29±1.44	73.63±0.87	74.39±0.92	74.75±1.57	76.15±1.34
320	77.20±0.84	72.73±1.58	75.12±1.15	75.88±0.83	77.24±1.91	77.78±1.00	77.22±1.13	78.54±0.51
360	78.28±0.64	74.97±1.68	76.35±1.17	77.97±0.36	78.22±0.64	78.60±0.92	78.44±1.21	79.67±0.62
400	77.01±1.22	73.70±1.72	75.38±0.64	76.62±0.88	77.35±0.88	77.27±1.09	77.25±1.38	79.05±0.17